Fracture Load Predictions — How Accurate?

L.N. Gifford, E.J. Czyryca
David W. Taylor Naval Ship Research and Development Center, Bethesda, Maryland 20084, U.S.A.

SUMMARY

A critical look is taken at the application of the principles of linear and nonlinear fracture mechanics for the prediction of fracture loads for simple fillet fatigue specimens tested under load control. Specimens were fabricated from both brittle and ductile materials, for which critical values of the stress intensity factor (K_{IC}) and the J-integral (J_{IC}) respectively were used as fracture criteria.

Although the geometry of these specimens was rather simple, cracks were formed under corrosion fatigue, initiating at a number of sites. Thus the crack depths at fracture were irregular across the specimen thickness. Fracture load ranges based on deepest and shallowest crack depths were too broad to be of engineering significance. An "effective" uniform crack depth was assumed for two-dimensional fracture load computations by finite element and other methods. This paper addresses this aspect of the problem by comparing experimental fracture loads with predicted loads calculated under various assumptions, and draws conclusions as to suitable ways to obtain conservative but reasonably accurate predictions.

Other factors associated with fracture load prediction are also discussed. These include accuracy loss due to small errors in measured or assumed crack depth, conditions under which plastically corrected linear elastic solutions can be used for nonlinear problems, the consequences of using two-dimensional models for three-dimensional problems (and the frightening implications for more complex structures), and the possible consequences of attempting to correct a fracture problem by simple substitution of a tougher material.

1. Introduction

The prediction of fracture loads for cracked structures or, conversely, the prediction of crack size necessary for fracture at a given load, is more difficult in practical engineering than for the simple cases described in theoretical fracture mechanics. Accurate prediction, however, is the aim of quantitative fracture mechanics. This paper describes the application of both linear and nonlinear fracture mechanics principles to predict fracture loads for nonsymmetric simple specimens. The results are examined from a practical viewpoint, i.e. the effects of engineering judgement and simplifying assumptions on the accuracy of predictions are examined.

A number of small fillet fatigue specimens as shown in Figure 1 were manufactured from both brittle and ductile alloys. The specimens were fatigue tested to failure under load control in a corrosive medium by the second author. Mechanical and fracture properties, and the final fatigue crack profile were then submitted to the first author for the prediction of fracture loads. The objective of the work was thus to examine predictive capability in an environment unbiased by foreknowledge of the experimental fracture loads.

2. Experimental Program

2.1 Materials

The two alloys used in this study were a high-strength, quenched and tempered steel (AISI 4150H), and a high strength, age hardening, nickel base alloy (Inconel 718, Ni-18Fe-19Cr-3Mo-5Cb-1Ti). Both materials were received as large diameter ring forgings approximately 150mm (6 in.) in thickness. For the 4150H steel, Young's modulus was measured as $2x10^{11}$ pa ($29x10^{6}$ psi), the 0.2 percent offset yield stress was 751 Mpa (109 ksi), and Poisson's ratio was 0.33. Corresponding properties for Inconel 718 were $2x10^{11}$ pa ($29x10^{6}$ psi), 994 Mpa (144 ksi), and 0.33 respectively. The orientation of all test specimens was such that the plane of fracture was in the through-thickness direction of the forgings. The tensile properties were obtained by ASTM Standard Method E8, reaching load and strain well beyond yield to determine the strain hardening slope. For Inconel 718, it was found that the stress-strain curve could be approximated by a bilinear model with a yield stress of 994 Mpa (144 ksi) and a strain hardening slope of $1.24x10^{10}$ pa ($1.8x10^{6}$ psi).

2.2 Fracture Toughness Tests

The fracture toughness of the brittle alloy, 4150H steel, was determined using fatigue precracked compact specimens and the procedures given by ASTM standard E399. K_{IC} determined from these tests met all validity requirements and averaged 60.6 Mpa$\sqrt{m}$ (55 ksi $\sqrt{in.}$) Charpy V-notch energy was found to be 14.9J (11 ft.-lb.).

The fracture toughness of the ductile Inconel 718 was characterized by means of J-integral methodology using a modified fatigue precracked specimen. The test procedure [1] determines J_{IC} for a single specimen by means of a computer-interactive testing system which monitors instantaneous values of crack length, area under the load-displacement curve, and geometry factors. J_{IC} values were computed from the intersection of the crack opening stretch line (blunting line) and the straight line R-curve fit, and were found to average 150 KJ/m^2 (855 in.-lb./in.^{2}). Charpy V-notch values averaged 61J (45 ft.-lbs.).

2.3 Fillet Fatigue Tests

The fatigue specimens were subjected to combined static and cyclic loading in a Sonntag-type fatigue machine as shown schematically in Figure 1. The machine applied a constant amplitude load by a mechanical oscillator at a frequency of 30 Hz and automatically maintained constant static load. The load was transferred to the specimen via a spherical seat nut and washer to allow for bending of the loading arm. A plastic well was attached to the specimen in the region of the fillet, through which aerated, natural seawater was pumped at about 50 ml/min.

Failure in the fatigue tests was by complete fracture of the specimen at maximum static and dynamic load. After failure, the fatigue crack depth and angle was carefully measured at the edges, the quarter points, and the center (five places). Results of these measurements are given in Table I, and the crack profiles are shown to scale in Figure 2. Corrosion-fatigue cracks initiated at several origins along the fillet on most specimens. Thus the final depth of crack at fracture was that of multiple joined cracks, irregular, and representative of a "real" crack front.

3. Computational Program

3.1 Two-Dimensional Linear Elastic Computations

Initial elastic fracture computations for the brittle 4150H steel specimens were performed with the APES finite element computer program [2]. This program employs a high order 12-node isoparametric element. Special 12-node enriched elements [3] containing the additional elastic singular solution are used about the crack tip such that the modes I and II stress intensity factors are included as unknowns in the formulation. Accuracy has been found to be excellent, even when very coarse meshes are used and large elements surround the crack tip [4] such as shown in Figure 1. The APES program is capable of plane strain, plane stress, or axisymmetric fracture analysis.

The fillet fatigue specimens are not symmetric with respect to the fillet region and, indeed, fatigue crack growth was not exactly perpendicular to the applied bending stress field. Thus there was some initial concern over combined mode effects on the fracture process. A number of plane strain finite element computations were performed to determine the relative magnitudes of the stress intensity factors K_I and K_{II} as a function of crack angle and crack depth. It was found in all cases that K_{II} was negligibly small. K_I and K_{II} are compared in Figure 3 (triangular points) for a vertical crack orientation for various values of the crack depth to width ratio, a/w.

The small amplitude of the mode II stress intensity factor suggested that the failure occurs in a symmetric mode despite the asymmetrical nature of the specimens. This was verified by finite element models of the specimen which included only the loaded end with a plane of symmetry located along the crack plane. In these cases, values of K_I agreed quite closely with those calculated by modeling the whole specimen, and are shown as circles in Figure 3. More importantly, it was found that these stress intensity factors agreed quite well with handbook values if the crack depth was assumed to be the sum of the fatigue crack depth and the notch depth. The handbook values are shown as a solid line in Figure 3.

Thus for the linear elastic case, the stress intensity factor can be calculated in closed form as

$$K_I = \frac{6M}{W^2} \sqrt{\pi a} \quad F(a/w) \qquad (1)$$

where M is the applied moment, W is the specimen width, a is the sum of the notch depth and crack depth and F(a/w) is given by Tada [5]. While this discovery may not seem surprising, it nonetheless should not have been assumed until verified by finite element calculations, nor is this simplification helpful in dealing with cracks whose depth varies across the thickness of the specimen. Finally, it is important to note that crack depths of interest in this study have high ratios of a/w which correspond to the very steep portion of the curve in Figure 3. Thus small differences in assumed crack depth lead to big differences in the applied stress intensity factor.

3.2 Two-Dimensional Elastic-Plastic Computations

For the ductile Inconel 718 specimens, finite element analyses were necessary to evaluate the integral equation given by Rice [6] for the path value of the J-integral as a function of applied load. This was accomplished through an extension of the APES code, called PAPST, which incrementally solves the elastic-plastic fracture problem. Again, 12-node isoparametric elements are used, and the Hutchinson-Rice-Rosengren singularity [7,8] is built into elements which surround the crack tip. The J-integral is numerically evaluated at each load step over a number of user-specified paths about the crack tip. The "best" path was chosen as that which agreed most closely with the linear elastic K_I solution at the load corresponding to first yield. Within the linear range and under conditions of plane strain, J and K_I are related by

$$J = \frac{K_I^2 (1-\nu^2)}{E} \tag{2}$$

where ν is Poisson's ratio and E is Young's modulus.

The fact that a formula for the stress intensity factor, eq. (1), fit the finite element results in the linear elastic range suggested that a plastically corrected elastic solution might also be used to calculate J for the ductile specimens. The plasticity correction is quite simple as outlined by Broek [9]. K_I is first calculated (for a given load) by eq. (1), and then the radius of the plastic zone at the crack tip, r_p is approximated (for plane strain) as

$$r_p = \frac{1}{6\pi} \left(\frac{K_I}{\sigma_y}\right)^2 \tag{3}$$

where σ_y is the material yield stress. An "effective" crack depth a' is then estimated as

$$a' = a + r_p \tag{4}$$

and the result is substituted back into eq. (1) to yield a corrected (higher) value for K_I. The J-integral is then calculated using eq. (2). The procedure is repeated for a sequence of increasing loads until the desired range of load versus J is covered.

It is noted that a simplification of this type (using linear solutions to generate non-linear solutions) is not practical unless a simple closed form solution exists for the stress intensity factor. Without such a solution, nonlinear finite element analysis is more practical, since otherwise at least one different elastic finite element solution would be necessary for each load step. Moreover, the procedure is not always applicable.

4. Numerical Results

4.1 Linear Elastic Computations

Initial fracture load computations were performed for six crack depths for each of the brittle 4150H steel specimens. These depths corresponded to the two edge depths, the two quarter point depths, the center depth, and a depth equal to the average of these five measured depths. Eq. (1) was used to calculate the stress intensity factor, and K_{IC} was used to predict the fracture loads. These predictions, together with relevant specimen geometry, are shown in Table I.

4.2 Nonlinear Computations

For the nonlinear, ductile, Inconel 718 specimens, J versus applied load was calculated using linear elastic fracture mechanics, linear elastic fracture mechanics with a plasticity correction, and by a direct nonlinear finite element J-integral analysis. Again, computations were made for six different crack depths for each specimen. The results for all three solution methods for a typical specimen and typical crack depth are shown in Figure 4.

Two important facts emerge from this figure. First, assuming a value of J_{IC} of 150KJ/m^2 (855 in.-lb./in.^{2}), a linear elastic solution leads to considerably higher fracture load predictions, i.e. unconservative. Secondly, for J_{IC} below 160KJ/m^2 (900 in.-lb./in.^{2}), the finite element solution and the plastically corrected elastic solution are in close agreement. This trend was observed for all specimens. Above this value of J_{IC}, on the other hand, the plastically corrected linear solution becomes increasingly unconservative. Nonetheless, for the Inconel 718 material under study here, J values derived from a plastically corrected linear solution appear to be just about as good as those calculated by more expensive finite element analysis. Such a finding could not have been assumed, however; it had to be demonstrated by finite element computations. Fracture load predictions for the Inconel 718 specimens, based on the plastically corrected elastic solution for J, are shown in Table I.

4.3 Prediction and Comparison with Experiment

The ranges of predicted fracture loads for all specimens based on six assumed crack depths are indicated in column 3 of Table II. These ranges are obviously too broad to yield a fracture load of engineering accuracy, forcing one to rely on engineering judgment in order to estimate a fracture load. For lack of a more appealing assumption, the "first estimate" of fracture load was taken as the calculated load corresponding to the deepest quarter point crack depth, as shown in column 5 of Table II. The actual experimental loads were then revealed, indicating that these estimates ranged from 11 to 58 percent too low. This was not terribly pleasing, although the authors were happy that the experimental fracture loads at least fell within the calculated range.

With the experimental loads known, it became possible to compare various methods (assumptions) which might lead to more accurate fracture load predictions. Among methods compared were:

(a) Crack depth = deepest quarter point depth.

(b) Crack depth = center point depth.

(c) Crack depth = shallowest quarter point depth.

(d) Crack depth = average of center, quater point, and edge depths on the most deeply cracked side of the specimen.

(e) Crack depth = average of center and quarter point depths.

(f) Crack depth = average of all five measured depths.

The results of these computations are shown in Table III, which demonstrates that conservative or nonconservative fracture loads can be calculated depending on the effective crack depth chosen. Of the different methods shown, method (e) appears to work best for the brittle specimens. The errors range from 6 percent high to 33 percent low. For the ductile specimens, method (d) apparently works best, with errors of +2 and -6 percent. Results based on these two methods have been entered in Table II as the "second estimate" fracture loads.

From the results in Table III, it is impossible to say with any certainty that one method of fracture prediction is clearly superior to the others. There are two reasons for this. First, although all cracks were uneven in depth, the nonuniformity differed from specimen to specimen. Thus a predictive approach that works well for one specimen will not work as well for another. Second, small errors in measurement of the crack depth can lead to large changes in the predicted fracture load. For example, the fracture load predicted for specimen FDY-510 for a crack depth of 9.78 mm (0.385 in.) is 3690 N (830 lbs.) and is 4 percent too high. If, on the other hand, the crack depth were actually 9.53 mm (0.375 in.), a measurement error of only 0.25 mm (0.01 in.), the predicted fracture load would be 3960 N (890 lbs.) which is 11 percent too high. An even larger difference for a similar measurement error results for the ductile Inconel 718 specimens. In light of these factors, the accuracies achieved in Table II, especially for the blind "first estimate", could be considered surprisingly good.

5. Observations and Discussion

Linear elastic fracture mechanics principles can, of course, be used to predict fracture loads for brittle 4150H steel fillet fatigue specimens using K_{IC} fracture criterion. Nonlinear fracture mechanics principles (direct nonlinear finite element calculation of the J-integral, or calculation of J based on a plastically corrected elastic solution) were used to predict fracture loads for ductile Inconel 718 specimens. In the presence of a nonuniform crack depth, the accuracy of all predictions depended on the assumed effective crack depth. The effective crack depth for brittle and ductile fracture specimens must apparently be chosen differently for most accurate fracture load predictions. Conservative fracture load predictions were obtained for both alloys by taking the effective crack depth as that at the deepest quarter point.

Regarding nonlinear computations, linear elastic fracture mechanics formulas to which a plasticity correction can be applied exist only for simple geometries. The plasticity correction approach as used here does not account for strain hardening. As the strain hardening slope increases, the value of J at a given load actually decreases. Thus for materials having significant strain hardening, the approach leads to overly conservative fracture load predictions. In sum, the applicability of the plasticity correction approach is dependant on a contained plastic zone, cracks which are neither too shallow or too deep, the availability of a formula for the stress intensity factor, a sufficiently small value of the J_{IC} to yield stress ratio, and a sufficiently small slope of the hardening portion of the stress-strain curve.

Even if the cracks had been of uniform depth, this work indicates that accuracy in measuring the crack depth is more important in predicting fracture loads than is a precise measure of the material properties K_{IC} and J_{IC}. In this experiment accurate measurement of the crack depth was made from the broken specimens before making fracture load predictions. In the real world, crack depths cannot generally be obtained so precisely.

In all of this work, an attempt has been made to solve fracture problems which are actually three-dimensional by the use of two-dimensional computations and an assumption for the effective crack depth. Preliminary three-dimensional elastic finite element computations have revealed that the variation of the stress intensity factor across the thickness of unevenly cracked specimens is not as great as indicated by the two-dimensional results, especially in the central three-quarters of the specimens. Thus three-dimensional computations, although much more expensive, can be expected to give fracture load predictions which are more accurate.

Finally, it is of interest to compare the fracture response of nominally identical cracked specimens made of brittle and ductile materials, the objective being to obtain some insight into what is gained by replacing a brittle material with a ductile material. Using the inverse of eq. (2) to obtain an approximate K_{IC} for Inconel 718 from its J_{IC} value, one obtains K_{IC} = 182 Mpa$\sqrt{m}$ (166 ksi $\sqrt{in.}$), which is about three times higher than that of 4150H steel. Since the applied stress intensity factor is directly proportional to the applied load, one might expect the ductile specimen to carry about three times the load of the brittle specimen if all dimensions and crack depths are the same. Of the brittle and ductile specimens tested, the two most nearly identical in crack depth, width, and the ratio of crack depth to width are FDY-512 and FFZ-58. The ductile specimen is not quite as severely cracked as the brittle specimen and, according to fracture toughness arguments, should carry a considerably higher load than the brittle specimen without fracturing. The ratio of the experimental fracture loads, however, was 1.7 rather than 3. The reason for this big difference, of course, is due to the plastic flow which develops in the ductile specimen. Because of these circumstances, it is highly unconservative to apply linear elastic fracture mechanics principles to ductile materials. Results such as these should be weighed carefully when one contemplates the correction of a fracture problem by changing materials to increase fracture toughness; the gain may be much less than expected. The best course of action, as always, is to avoid crack formation and/or growth altogether by proper design and quality control.

Acknowledgment

The authors thank Dr. Hans H. Vanderveldt of the Naval Sea Systems Command, and Mssrs. John P. Gudas and Archie J. Wiggs of the David Taylor Naval Ship Research and Development Center for their support of this work.

References

[1] JOYCE, J.A., GUDAS, J.P., "Computer Interactive J_{IC} Testing of Naval Alloys", Elastic-Plastic Fracture, American Society for Testing and Materials STP668, 451-468 (1979).

[2] GIFFORD, L.N., "APES-Finite Element Fracture Mechanics Analysis: Revised Documentation", David Taylor Naval Ship Research and Development Center Report 79/023 (March, 1979).

[3] BENZLEY, S.E., "Representation of Singularities with Isoparametric Finite Elements", Int. J. for Numerical Meth. in Engng., 8, 537-545 (1974).

[4] GIFFORD, L.N., HILTON, P.D., "Stress Intensity Factors by Enriched Finite Elements", Engng. Fracture Mech., 10, 3, 485-496 (1978).

[5] TADA, H., The Stress Analysis of Cracks Handbook, Del Research Corporation (1973).

[6] RICE, J.R., "Mathematical Analysis in the Mechanics of Fracture", in Fracture, 2, Academic Press (1968).

[7] HUTCHINSON, J.W., "Singular Behavior at the End of a Tensile Crack in a Hardening Material", J. Mech. and Physics of Solids, 16, 1 (1968).

[8] RICE, J.R., ROSENGREN, G.F., "Plane Strain Deformation Near a Crack Tip in a Hardening Material", J. Mech, and Physics of Solids, 16, 1 (1968).

[9] BROEK, D, "Elementary Engineering Fracture Mechanics", Noordhoff Int. Publishing, Leydon (1974).

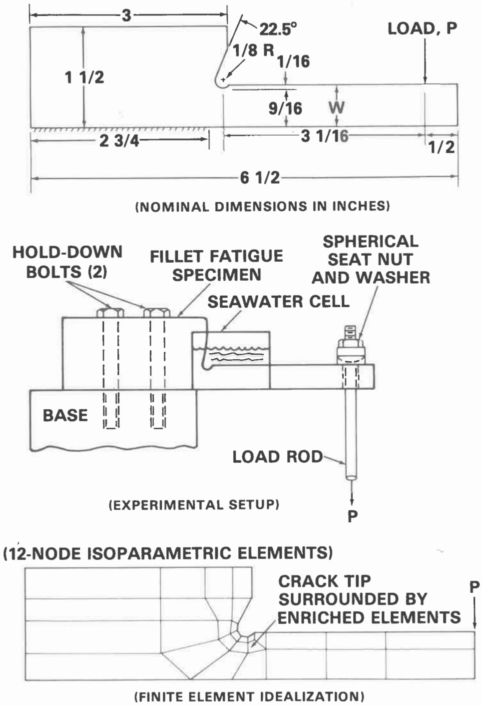

Figure 1 - Geometry, Experimental Setup, and Idealization of Fillet Fatigue Specimens

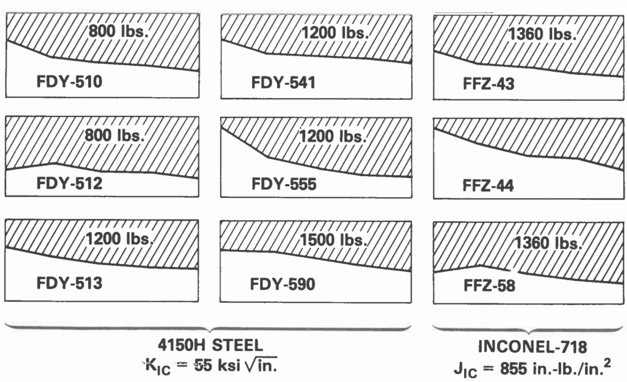

Figure 2 - Crack Profiles at Fracture and Fracture Loads for Fillet Fatigue Specimens

TABLE I - SUMMARY OF FRACTURE LOAD COMPUTATIONS

SPECIMEN	MAT'L.	THICKNESS B (IN.)	WIDTH W (IN.)	CRACK DEPTH* (IN.) AND CALCULATED FRACTURE LOAD (LBS.)					
				EDGE	QUARTER POINT	CENTER	QUARTER POINT	EDGE	AVERAGE
FDY-590	4150H STEEL	1.510	0.6175	0.225 1740	0.235 1670	0.295 1270	0.351 950	0.382 780	0.2976 1250
FDY-541	↓	1.505	0.6225	0.189 2060	0.299 1270	0.317 1160	0.332 1080	0.363 900	0.2998 1270
FDY-555	↓	1.500	0.6125	0.065 3590	0.299 1210	0.382 750	0.437 500	0.450 440	0.3266 1050
FDY-513	↓	1.503	0.6225	0.234 1700	0.299 1270	0.350 970	0.373 850	0.384 790	0.3280 1100
FDY-510	↓	1.490	0.6325	0.213 1920	0.351 1010	0.385 830	0.410 710	0.446 540	0.3610 960
FDY-512	↓	1.493	0.6155	0.425 560	0.361 870	0.428 550	0.427 550	0.481 330	0.4244 560
FFZ-44	INCONEL 718	1.485	0.6375	0.389 1920	0.302 3210	0.284 3500	0.188 5350	0.070 8850	0.2466 4160
FFZ-43	↓	1.491	0.6405	0.470 1010	0.441 1330	0.395 1890	0.374 2170	0.270 3810	0.3900 1950
FFZ-58	↓	1.498	0.6375	0.477 920	0.452 1180	0.398 1820	0.337 2680	0.396 1850	0.4120 1640

*CRACK DEPTH PLUS NOTCH DEPTH.

TABLE II - COMPARISON OF CALCULATED AND EXPERIMENTAL FRACTURE LOADS

SPECIMEN	MATERIAL	CALCULATED FRACTURE LOAD RANGE (LBS.)	EXPER. FRACTURE LOAD (LBS.)	FIRST ESTIMATE* FRACTURE LOAD (LBS.)	PERCENT ERROR	SECOND ESTIMATE FRACTURE LOAD (LBS.)	PERCENT ERROR
FDY-590	4150 H STEEL	780-1740	1500	950	-37	1280	-15
FDY-541	↓	900-2060	1200	1080	-10	1170	-2
FDY-555	↓	440-3590	1200	500	-58	800	-33
FDY-513	↓	700-1700	1200	850	-29	1030	-14
FDY-510	↓	540-1920	800	710	-11	850	+6
FDY-512	↓	330-870	800	550	-31	650	-19
FFZ-44	INCONEL 718	1920-8850	**	3210			
FFZ-43	↓	1010-3810	1360	1220	-11	1390	+2
FFZ-58	↓	920-2680	1360	1100	-19	1280	-6

*BASED ON CRACK DEPTH AT DEEPEST QUARTER POINT.
**LOAD NOT KNOWN; FAILURE DUE TO ACCIDENTAL OVERLOAD.

TABLE III - FRACTURE LOAD AND ERRORS FOR VARIOUS PREDICTIVE METHODS

SPECIMEN	EXPER. FRACTURE LOAD (LBS.)	CALCULATED FRACTURE LOAD (AND PERCENT ERROR)					
		METHOD (a)	METHOD (b)	METHOD (c)	METHOD (d)	METHOD (e)	METHOD (f)
FDY-590	1500	950 (-37)	1270 (-15)	1670 (+11)	990 (-34)	1280 (-15)	1250 (-17)
FDY-541	1200	1080 (-10)	1160 (-3)	1270 (+6)	1050 (-12)	1170 (-2)	1270 (+6)
FDY-555	1200	500 (-58)	750 (-37)	1210 (+1)	560 (-53)	800 (-33)	1050 (-12)
FDY-513	1200	850 (-29)	970 (-19)	1270 (+6)	870 (-28)	1030 (-14)	1100 (-8)
FDY-510	800	710 (-11)	830 (+4)	1010 (+26)	690 (-14)	850 (+6)	960 (+20)
FDY-512	800	550 (-31)	550 (-31)	870 (+9)	470 (-41)	650 (-19)	560 (-30)
FFZ-44	UNKNOWN	3210	3500	5350	—	—	4160
FFZ-43	1360	1220 (-11)	1890 (+39)	2170 (+60)	1390 (+2)	1780 (+31)	1950 (+43)
FFZ-58	1360	1100 (-19)	1820 (+34)	2680 (+97)	1280 (-6)	1850 (+36)	1640 (+21)

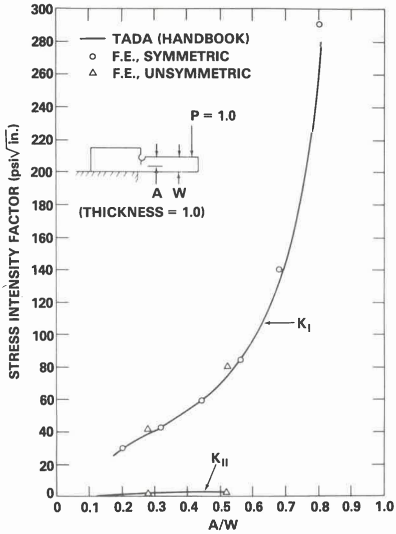

Figure 3 - Normalized Stress Intensity Factors versus Nondimensional Crack Depth for Typical Fillet Fatigue Specimen

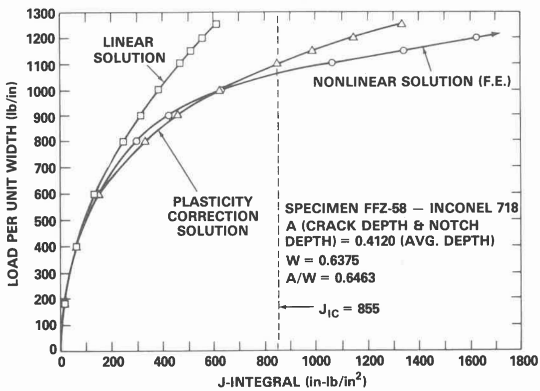

Figure 4 - J versus Load by Different Solutions for Inconel 718 Specimen FFZ-58